

Wi-Fi RF Energy Harvesting for Battery-Free Wearable Radio Platforms

Vamsi Talla^{*,†}, Stefano Pellerano[†], Hongtao Xu[†], Ashoke Ravi[†] and Yorgos Palaskas[†]

[†]Intel Corporation, Hillsboro, OR 97124

^{*}Department of Electrical Engineering, University of Washington, Seattle, WA 98195

Email: vamsit@uw.edu, {stefano.pellerano, hongtao.xu, ashoke.ravi, yorgos.palaskas}@intel.com

Abstract—Wearable devices have huge market potential, but their usage has been limited because means to power such devices is still a challenge. Batteries, the most widespread solution, add size, weight and need periodic recharging which is a huge deterrent. In this work, we propose to eliminate batteries by leveraging Wi-Fi transmissions from nearby devices such as access points and smart phones to deliver power wirelessly to wearable devices.

We develop a wearable temperature sensor, which harvests energy from Wi-Fi transmissions and transmits data back to an access point. We enable this application by designing an efficient 2.4 GHz Wi-Fi harvesting front-end to power an ANT radio platform with a smartphone as the Wi-Fi source. We study and analyze the effect of OFDM modulation, wide bandwidth (72 MHz) and the bursty nature of 802.11 Wi-Fi signals on the sensitivity, efficiency and the output power of the RF harvester. Our prototype achieves a sensitivity of -16.5 dBm with 100 % duty cycle Wi-Fi transmissions for a target output voltage of 2.05 V and 2.5 μ W leakage at the storage capacitor node. This translates to an operating range of about 11.5 cm from a 2 dBm Wi-Fi transmitter on a smartphone and 92 cm from a 20 dBm Wi-Fi access point with a 3 dBi antenna on the wearable device.

I. INTRODUCTION

Wearable devices are tiny computation and sensing platforms worn on the body to provide means to periodically track, store and process key physiological parameters, human activity and events [1]. A growing number of health, fitness and wellness applications are using wearable devices such as smart watches, FitBit, Jawbone [2]–[4]. Since wearable devices are mobile and worn on the body, they are required to be small, light, inconspicuous and easy to use and maintain.

On a very high level, wearable devices contain three main components: a computation core, sensor(s) and means for wireless communication. Technology improvements in all these domains have enabled the proliferation of wearable devices by making them smaller, lighter, more functional and power efficient. CMOS scaling, a consequence of Moore’s law is enabling smaller, faster and increasingly power efficient digital platforms [5]. Micro-fabrication techniques (MEMS) is leading the way to small and power efficient sensors [6]. Evolving manufacturing, assembly and integration techniques are enabling smaller, lighter and more cost-efficient devices.

However, in spite of all these advancements, limitations in sources of power have hindered the widespread acceptability and usage of wearable devices. Battery technology hasn’t scaled and as a consequence, the current approach of using

batteries adds cost, size and weight [7]. Batteries have a limited life span and require periodic recharging and replacement, which is a huge deterrent. As the wearable devices scale in numbers and attempt to gain wider acceptability and usage models, there is a need for alternate mechanisms to power these devices. Radio communication is the major power contributor in typical platforms [8] and in this work, we focus on using energy harvesting to power a radio and eliminate batteries on wearable platforms.

Over the years, solar, thermal, motion and RF power harvesting have been investigated for battery-free sensing and computation [7], [9]–[14]. In this work, we will focus on harvesting energy from RF sources since we believe; this approach has several advantages for wearable devices. All devices require an antenna for communication, in principle, the same antenna can be utilized to harvest incoming RF power. On the other hand, solar, thermal and motion based harvesting need additional transducers, which increase size and weight, and is prohibitive for wearable devices. Additionally, wearable devices are extremely mobile and, the output power of solar, thermal and motion based harvesting is inconsistent and unpredictable due to the dependence on external factors such as light, temperature and human movement respectively. On the other hand, on a daily basis, we are consistently surrounded by RF signals such as cellular, TV and Wi-Fi, which are potential means to power tiny wearable devices [15]. In the next section we will explore the applicability of the various RF signals as a source of power for wearable devices.

II. RF POWER HARVESTING FOR WEARABLE DEVICES

Ambient RF signals such as TV and cellular transmissions from base stations are ideal candidates. However, wearable devices are primarily used in indoor environments such as offices and homes. The typical power level of ambient RF signals indoors is too low for RF energy harvesting and as a result, impractical for powering wearable devices.

Wearable devices are extremely power constrained and to minimize power associated with wireless communication (the major contributor), they operate in close proximity to an access point such as a smartphone. Such devices use short-range energy-efficient wireless protocols such as ANT and BLE to communicate with the access point. On the other hand, access points such as smartphone and tablets have a reasonably sized battery and are recharged periodically. We can leverage this

close proximity to eliminate the battery on the wearable device and instead deliver power from the access point to the wearable device using a dedicated wireless link.

Access points such as smartphones/tablets transmit RF energy in a wide range of frequency bands such as 2G, 3G, LTE, HSPA cellular bands and 2.4 and 5 GHz Wi-Fi. However, cellular transmissions only occur when there is an active phone call or text or data transmission. Additionally, the handset has little control over transmit power since it's dictated by the base station based on the handset's location [16]. As a result, the power transmitted by the phone is unpredictable and location dependent, making cellular harvesting is too inconsistent for powering wearable devices.

Wi-Fi at 2.4 GHz is nowadays ubiquitous in all hand-held devices like tablets and smartphones, which can be leveraged to deliver power. The wearable platform harvests power from 2.4 GHz Wi-Fi transmissions of a nearby access point and uses energy-efficient ANT protocol to transmit the sensor information to the access point.

A. Smartphone as the power source

Since smartphone is nowadays ubiquitous and commonly used access point for wearable devices, Wi-Fi transmissions from the smartphone can be used to deliver power. However, the output power of Wi-Fi transmission from a smartphone is low (around 0-2 dBm including antenna and enclosure losses) and this limits the operating distance between the smartphone and the wearable device. In order to maximize the operating range, we optimize the Wi-Fi harvester for sensitivity, i.e. the lowest power at which the harvester can operate. We develop a -16.5 dBm sensitivity harvester that can power an ANT radio and operate up to a distance of 11.5 cm from a 2 dBm Wi-Fi transmitter on a smartphone with a 3 dBi antenna.

B. Implications of harvesting Wi-Fi signals

In the United States, Wi-Fi operates in the 2.401 - 2.473 GHz spectrum with 802.11 b/g/n standards, which differ in modulation rates, spectral mask and data rates. The most popular Wi-Fi standard 802.11 g/n uses OFDM (orthogonal frequency division multiplexing) modulation in 20 MHz channels centered around 2412 MHz, 2437 MHz and 2462 MHz. OFDM signals have high peak to average power ratio which increases the rectifier efficiency, when compared to continuous wave transmissions [17], [18]. The impact of OFDM signals on the rectifier performance has not been evaluated in literature.

Unlike RFID and TV transmissions, which are continuous wave transmission, Wi-Fi uses carrier sense multiple access (CSMA) and a packet-based protocol resulting in bursty radio transmission. Therefore, the time averaged output power of Wi-Fi is a function of the network traffic. This phenomenon can be quantified in terms of duty cycle (i.e. fraction of time Wi-Fi signals occupy the channel) and should be taken into account to ascertain the available power on the wearable platform. Hence, the OFDM modulation and packet based protocol makes harvesting Wi-Fi signals a unique challenge compared to prior work on RFID and TV band power harvesting.

Prior work on RF harvesting in the 2.4 GHz frequency band has focused on harvesting power from continuous wave input instead of 802.11 Wi-Fi signals [19], [20]. Additionally, these systems have poor sensitivity and suffer from low efficiency at typical Wi-Fi power levels. Furthermore, these systems are only rectifiers, which output few 100s of mV , insufficient to power sensing and computational platforms. Recent work has considered the bursty nature of Wi-Fi on the performance of rectifier [21]. But, it is also just a rectifier and lacks the boost converter and power management required to power a radio platform. In [22] authors design a rectenna patch and power management solution for Wi-Fi harvesting, but the harvester suffers for poor sensitivity and efficiency. The authors characterized the rectenna (excluding the boost converter and power management) for continuous wave input and did not study the impact of Wi-Fi signals on energy harvesting. Additionally, they used an antenna array, which increases the size of the platform and is prohibitive for wearable applications.

The power associated with radio communication is typically high and requires a big storage element and optimized power management for efficient operation. This challenge has not been addressed in literature for Wi-Fi energy harvesting. In this work, we develop a 2.45 GHz Wi-Fi harvester to power an ANT radio platform. Our system described in Section III, achieves a sensitivity of -16.5 dBm with 100 % duty cycle Wi-Fi transmissions for a target output voltage of 2.05 V and $2.52 \mu W$ platform leakage at the output. We study and analyze the implication of Wi-Fi bandwidth (72 MHz), OFDM modulation and the bursty nature of Wi-Fi transmissions on the efficiency, sensitivity and the power available at the output of the harvester in Section IV.

III. DESIGN AND ARCHITECTURE OF THE WEARABLE PLATFORM

In this section, we discuss the design and implementation of a battery-free wearable platform, which uses harvested power from Wi-Fi to sense temperature and transmit the sensor data back to an access point using ANT radio protocol. All components of the wearable platform including power management, computational core, temperature sensor and the radio, are powered from harvested Wi-Fi signals.

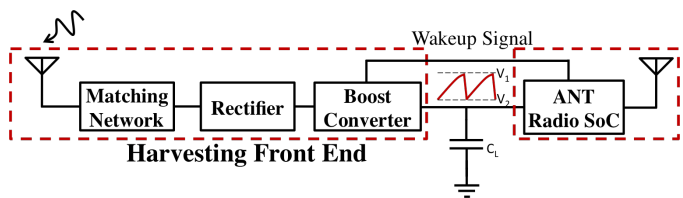


Fig. 1. The overall architecture of the Wi-Fi powered ANT radio wearable platform

Fig. 1 shows the architecture of the Wi-Fi powered wearable radio platform. The system consists of two main blocks: the harvesting front end (antenna, matching network, rectifier and a boost converter) and the ANT radio SoC. The RF signal is captured by the antenna and converted into DC power in a

two-step process: a single stage rectifier first converts the RF to low voltage DC and is then boosted to a higher voltage and stored on a capacitor [14]. The ANT SoC comprises of the computation core, temperature sensor and the radio and is powered by the boost converter. Note that in this prototype we use separate antennas for harvesting and communication. However, in principle since both Wi-Fi and ANT operate in the 2.4 GHz ISM band, a single antenna can be multiplexed (with additional 0.5 dB loss using a switch similar to [23]) between the harvesting and communication front end.

A. Design philosophy and metrics

The power available from Wi-Fi is typically very low (few μW), hence it is imperative that the platform is designed to maximize the harvested power and minimize the overall power consumption. To accomplish these two goals, the wearable platform operates on the principle of duty cycling. By default, it stays in a low power mode consuming minimal power (for state retention), efficiently harvesting power and accumulating charge on a capacitor. As soon as the capacitor has sufficient energy, the platform switches to an active mode, samples sensor data, encapsulates the sensor information in a packet, transmits the packet to the access point using ANT protocol and then transitions back to the sleep mode.

An RF powered platform has two main design metrics: the maximum operating range from the access point and the update rate of the sensor information, both of which are a function of harvesting efficiency and power consumption in the two modes of operation. Since the power available from Wi-Fi is very low, the platform spends majority of the time in the low power mode harvesting energy and occasionally goes to the high power mode. The power consumption in the low power mode, also known as the leakage of the platform, affects the harvesting efficiency and determines the maximum operating range from the power source. To maximize the operating range, the leakage of the platform should be minimized. Additionally, the average power consumption and the time spent in the high power mode (including radio transmission), determines the energy required for every active operation. This energy determines the update rate of the data transmissions, and should be minimized for high update rates.

B. Antenna

Wearable devices have stringent form factor constraints which limit the size and hence the gain and efficiency of the antenna. Furthermore, wearable devices are mobile and experience a great deal of variation in orientation and distance with respect to the access point. Hence, a directional antenna is not recommended. An inverted F antenna [24], a good trade-off between size, antenna gain and efficiency was chosen. The antenna measures 25.7 mm x 7.5 mm and has an efficiency and peak gain of 80% and 3.3 dBi respectively.

C. Matching Network and Rectifier

An RF rectifier is characterized by its efficiency and sensitivity. Efficiency at an input power is the ratio of the output

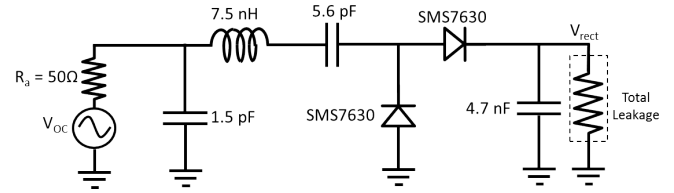


Fig. 2. The RF front end design of the rectifier to convert the Wi-Fi signal at 2.45 GHz into an output DC voltage.

DC power to the input RF power. Sensitivity is defined as the minimum input power at which, the rectifier can charge the storage capacitor to the target voltage. The efficiency and the sensitivity determine respectively, the update rate and the operating range of the wearable device. In this work, optimize the sensitivity of the rectifier to maximize the operating range.

Fig. 2 shows the one stage Dickson charge pump rectifier and the matching network used in this work. High RF to DC conversion efficiency is achieved by using low threshold voltage and junction capacitance SMS7630-061 schottky diodes [25] in the rectifier. Additionally, the miniature 0201 SMT packaged diodes minimize the losses associated with package parasitics. To minimize the power loss due to reflections at the antenna port, the rectifier front end is matched to the 50 Ω antenna using an LC match with high Q RF inductor and capacitor. The tuning of the front end was performed using a Vector Network Analyzer (VNA) and was optimized to achieve the lowest input power sensitivity. In the prototype implementation, we used a 7.5 nH series tuning inductor with a 1.5 pF parallel tuning capacitor.

The input impedance of the rectifier at -16 dBm continuous wave input across the frequency range of 2.401-2.473 GHz was measured using a VNA and is shown in Fig. 3 on a Smith chart. Fig. 4 plots the power reflected at the antenna interface as return loss and it can be seen that the matching is not optimal across the entire Wi-Fi bandwidth. This can be attributed to the fact that a single stage matching network with high Q is used for matching a large bandwidth signal (72 MHz wide) [26]. This variation in the input impedance results in variation in efficiency of the rectifier across the Wi-Fi channels and will be discussed in the section IV.

The efficiency and sensitivity of the rectifier at a given operating frequency are a function of the leakage power of the platform and the desired output voltage. In order to achieve high efficiency and sensitivity, the leakage of the platform was minimized. In this work, for a target output voltage of 2.05 V and 2.5 μW leakage at the output, we achieve a sensitivity of -16 dBm for a continuous wave input. This leakage includes the contributions of the DC-DC converter and the ANT radio SoC.

The matching network was designed and the sensitivity of the rectifier for a continuous wave input signal was evaluated using a VNA. However, 802.11n Wi-Fi transmissions use OFDM modulation, which have high peak to average power ratio. Since the rectification process is non-linear and diodes

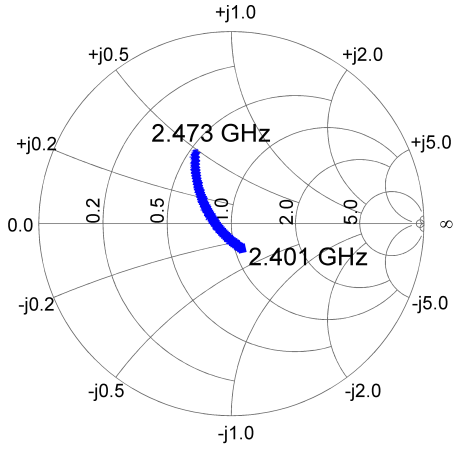


Fig. 3. Measured input impedance of the RF energy harvester for a -16 dBm continuous wave input across the Wi-Fi band.

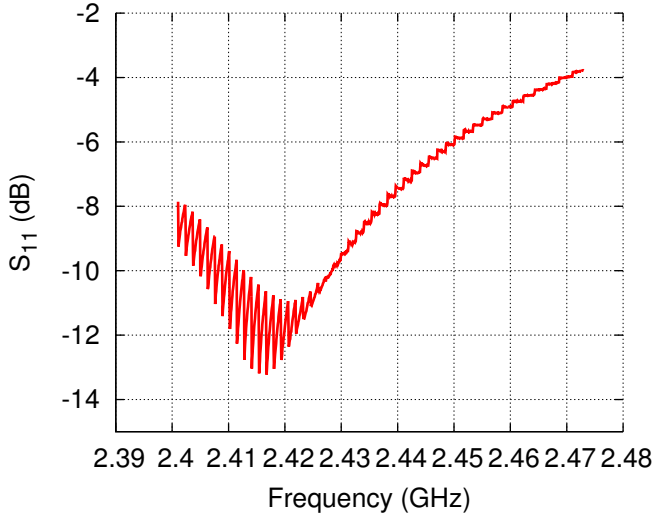


Fig. 4. Measured return loss at the input of the rectifier for -16 dBm continuous wave input across the Wi-Fi band. The ripple on the S_{11} is due to the switching in the boost converter which gets reflected on the input port of the RF harvester.

have a fixed voltage threshold, the performance of rectifier under excitation of signals with high peak to average power ratio will differ from continuous wave input [18]. We evaluate the impact of Wi-Fi transmissions on energy harvesting in Section IV.

D. DC-DC Converter

The low output voltage of the one stage rectifier stage is converted to the required voltage rail by the bq25570 energy harvesting solution [27]. bq25570 contains a high-efficiency boost converter, which can cold start from voltages as low as 330 mV and can operate from a 100 mV input once started. The boost converter also incorporates a voltage based maximum power point tracking (MPPT) mode (after cold start) [27]. Every 16 seconds, the boost is disconnected for 256 ms and the open circuit voltage is sampled and used as

a reference for MPPT. For example, the MPPT can be set to 80% or 50%, which regulates the input of the boost to 80% or 50% of the open circuit voltage respectively. However, this is impractical for Wi-Fi harvesting because Wi-Fi packets are non-continuous. If the open circuit sampling coincides with a period when there are no Wi-Fi packets, the sampled open circuit voltage is zero. This results in boost converter pulling the input to zero resulting in system failure. To mitigate this issue, a resistive divider between the output of the boost converter and ground was used to generate a reference voltage for the MPPT boost converter. For the one stage rectifier followed by the boost converter, 300 mV was found to be optimal MPPT reference voltage.

The bq25570 chip also contains a programmable voltage supervisor, which was used for duty cycle operation of the ANT SoC. The chip periodically measures (every 64 ms) the voltage on the storage capacitor and provides a wake-up signal when the voltage on the storage capacitor reaches the programmed threshold. In this work, we set the trigger threshold at 2.05 V. Please note that the wake-up signal is 64ms long, which has implications on the design of the ANT radio SoC.

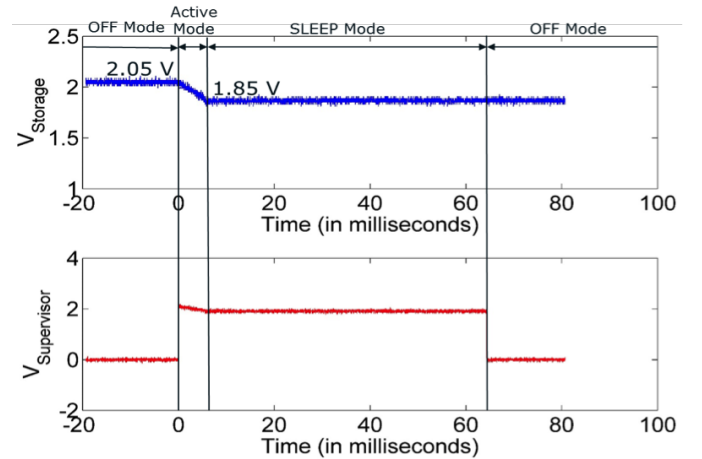


Fig. 5. The wakeup signal from the voltage supervisor of the bq25570 chip and corresponding voltage on the storage capacitor as a function of time. The various operating modes of the ANT SoC are annotated.

E. ANT Radio SoC

We used the nRF51422 ANT SoC, which contains an ARM core, a range of analog and digital peripherals, integrated temperature sensor, the ANT protocol stack and the radio front end [28]. The ANT protocol stack is incorporated as pre-compiled, pre-linked binary files called SoftDevice, which can be programmed into the SoC.

The ANT SoC transitions from the low power mode to the high power mode based on the wake-up signal from the supervisor in the bq25570 chip. This signal is typically 64 ms long and the ARM core in the SoC has unique interrupt characteristics, which necessitates the following configuration to minimize the leakage and active power consumption.

- By default the SoC operates in the OFF mode wherein it consumes only 350 nA of leakage current. It is configured to transition into active mode on a level-triggered input.
- When the voltage on the wake-up pin transitions to high, the SoC goes into ACTIVE mode. Since the SoC is transitioning from OFF mode, the CPU is reset. Upon wake-up, the CPU registers and the SoftDevice for the ANT protocol are initialized. A temperature sensor measurement is taken, encapsulated in a packet and transmitted using asynchronous ANT transmission to the access point. As soon as the transmission is complete, the SoC transitions to SLEEP mode. The SoC is configured to transition from SLEEP to OFF mode on the falling edge of the wake-up input from the voltage supervisor.
- In SLEEP mode, the SoC consumes 3.8 μA and stays in SLEEP mode as long as the wake-up signal is high (typically around 64 ms, which is the latency of the voltage supervisor). Once the falling edge on the wake-up pin is detected, the SoC transitions to OFF mode.

The wake-up signal and voltage of the storage capacitor corresponding to the different operating modes is shown in Fig. 5. We wrote an optimized firmware to minimize the energy consumption of one active mode operation (wake-up, temperature measurement, wireless transmission and going back to sleep) to 64 μJ . Based on this energy requirement and 1.8 V voltage minimum for the SoC, we chose a 160 μF storage capacitor and a wake-up threshold of 2.05 V. This resulted in a minimum voltage of 1.85 V (50 mV overhead) on the storage capacitor.

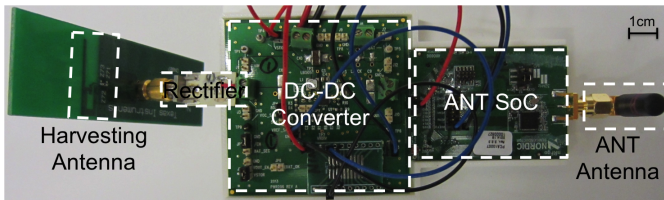


Fig. 6. The prototype implementation of the Wi-Fi powered wearable platform using off-the-shelf shelf components

We implemented the Wi-Fi powered wearable platform using commercial off-the-shelf components. The rectifier and matching network was custom designed on a low loss Rogers 4350 substrate and was interfaced with bq25570 and ANT SoC development boards. The developed prototype is shown in Fig. 6. The wearable platform cannot cold start from harvested Wi-Fi signals. This limitation is solely due to the start-up behavior of the ANT SoC. When the voltage at the input to the SoC rises slowly (slow charging of storage capacitor from harvested Wi-Fi power), the chip goes into an indeterminate state consuming large amount of current. This drains the energy from the storage capacitor and severely limits the harvester efficiency. As a compromise, we initiate a jump-start by connecting an external 1.8V voltage source to the storage capacitor. As soon as the storage capacitor is charged to 1.8V, the chip gets initialized, the 1.8V source is disconnected and the platform

runs continuously and sustains itself on harvested Wi-Fi power. Alternatively, a switchable element can be introduced between the storage capacitor and the ANT SoC to mitigate the ANT SoC startup issue. For example, an LDO (such as [29]) with enable functionality controlled by the supervisor output can be used to ensure that the ANT SoC connects to the storage capacitor only when the voltage is above 1.8 V.

IV. EXPERIMENTAL RESULTS

As explained in the previous section, the sensitivity and the efficiency of an RF energy harvesting front end is a function of input power, leakage of the platform and the desired output voltage. Hence, it is imperative that we evaluate the harvester taking into account all these factors. Additionally, unlike prior work, which focused only on the rectifier, here we evaluate the efficiency of the entire RF harvesting chain, i.e. rectifier and the DC-DC converter. The target output voltage is 2.05 V (required by the ANT SoC) on a 160 μF capacitor and the total leakage power of the entire wearable platform (2.5 μW) will be taken into account. To measure the efficiency and output power of the harvesting chain, we simply measure the time between successive active mode operations of the wearable platform. Since, each active mode operation requires 64 μJ , the time between successive operations is used to ascertain the average output DC power available for active mode operation.

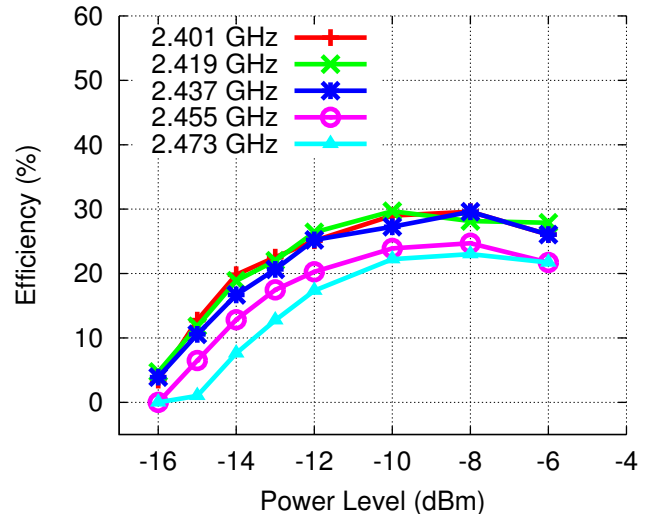


Fig. 7. The overall efficiency of RF harvester as a function of the operating frequency and input power for a continuous wave input.

A. RF harvesting with continuous wave input

First, we connect the rectifier front end to an RF signal generator and vary the input power and frequency of operation for a continuous wave signal. Fig. 7 shows the efficiency of the harvester as a function of the input power and operating frequency. It can be seen that the harvesting front end achieves a sensitivity of -16 dBm for a continuous wave input.

Additionally, as input power is increased, the harvesting efficiency first increases, reaches a maximum and then decreases. This phenomenon can be understood by noting that

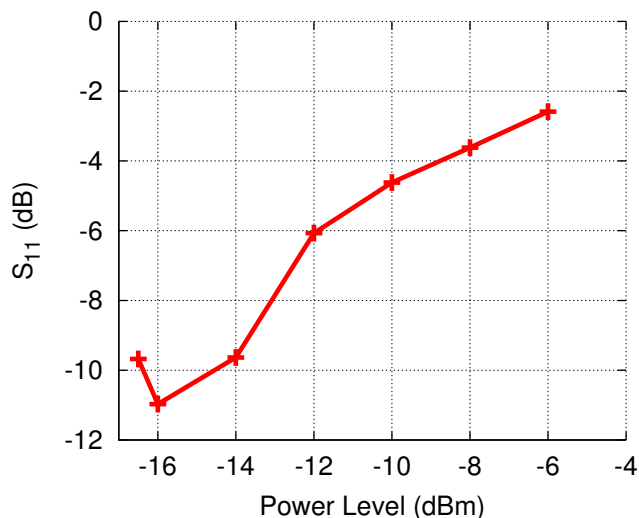


Fig. 8. The return loss at the antenna terminal of the RF front end as a function of the input power at 2.412 GHz continuous wave input.

the RF to DC efficiency depends on impedance matching (i.e. minimizing return loss at the antenna terminal) and RF to DC conversion of the rectifier charge pump. At low input power, the rectifier charge pump efficiency is low since the voltage levels are close to the threshold voltage of the diodes. As input power is increased, the voltage levels at the input of the rectifier charge pump increase leading to better rectification in the diodes of the charge pump. However, as seen in Fig. 8, as power increases, the impedance mismatch and hence losses due to reflection at the antenna terminal increase. This is a consequence of static impedance matching, optimized at a single input power of -16 dBm, which is the sensitivity of the rectifier. These two phenomena trade-off leading to lower efficiency at low input power (low efficiency of rectifier charge pump dominates), increased efficiency as input power is increased (higher efficiency of rectifier charge pump as voltage levels increase), with the maximum at -8 dBm and reduction in efficiency as losses due to impedance mismatch dominate.

Fig. 7 also shows that the efficiency of the harvester varies with operating frequency. The harvester has a better performance at 2.401, 2.419 and 2.437 GHz when compared to 2.455 and 2.473 GHz. This variation can be explained by noting that the front end is better matched at lower frequency than at higher frequencies as shown in Fig. 4.

B. RF harvesting with Wi-Fi as input

Next, we evaluate the performance of the harvester with Wi-Fi signals as input. A vector signal generator configured to transmit 4091 bytes long Wi-Fi packets with 64 QAM subcarrier modulation and no idle time (i.e. 100% duty cycle) was connected to the rectifier front end. The operating frequency and average power of the transmitted Wi-Fi packet were varied. Fig. 9 shows the efficiency as a function of input power for the three Wi-Fi channels (Channels 1, 6 and 11). When compared to the efficiency for continuous wave input

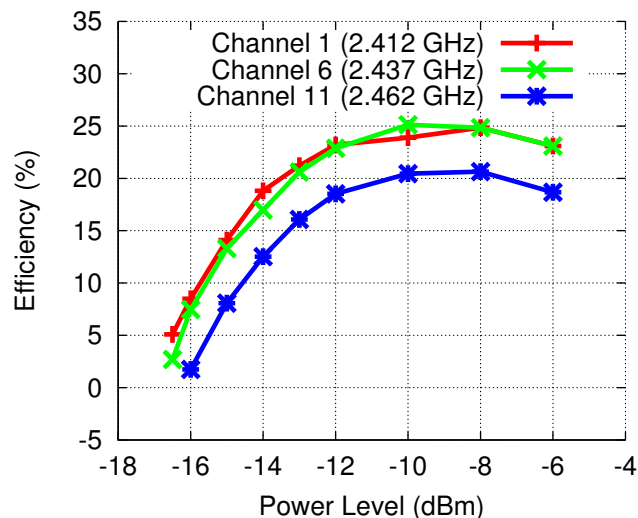


Fig. 9. Efficiency of the RF harvester for an input Wi-Fi signal and variation as a function of the Wi-Fi channels

(Fig. 7), the efficiency under OFDM signals is lower at high input power, but higher at low input power, which can be explained as follows. At high input power, the voltage at the diode for continuous wave input has already crossed the threshold of the diodes in the charge pump. The high peak to average power ratio of 64 QAM OFDM modulation results in peaks and valleys. But since diode conduction is exponential, the losses due to valleys do not compensate for the gains due to the peaks, which results in lower efficiency at high input power when compared to continuous wave input. But as the input power is reduced, the voltage levels are closer to the threshold of the diode and the gains due to the peaks supersede the losses due to valleys, leading to higher efficiency at lower input power. As a result, the sensitivity of the rectifier increases to -16.5 dBm for OFDM modulated Wi-Fi transmissions.

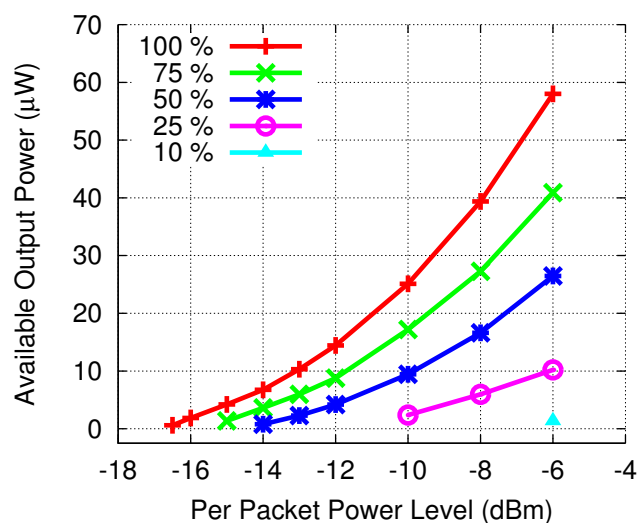


Fig. 10. Output power of the RF harvester as a function of the duty cycle and input power for Wi-Fi transmissions in Channel 6 of the 2.4 GHz Wi-Fi.

C. RF energy harvesting as a function of Wi-Fi duty cycle

Finally, we use the same vector signal generator setup and vary the duty cycle of Wi-Fi transmissions on Channel 6 (2.437 GHz). Fig. 10 shows the available DC power at the output of the RF harvesting chain as a function of the duty cycle of Wi-Fi transmissions. The x-axis plots the per packet power of the Wi-Fi transmissions. It can be seen that as the duty cycle of Wi-Fi transmission is reduced, the power at the output of the rectifier is also reduced, which leads to lower sensitivity, shorter operating range and slower update rates. This can be intuitively understood by noting that the leakage power of the platform is constant ($2.5 \mu W$) whereas as the duty cycle scales down the average input power linearly reduces, resulting in lower power available at the output.

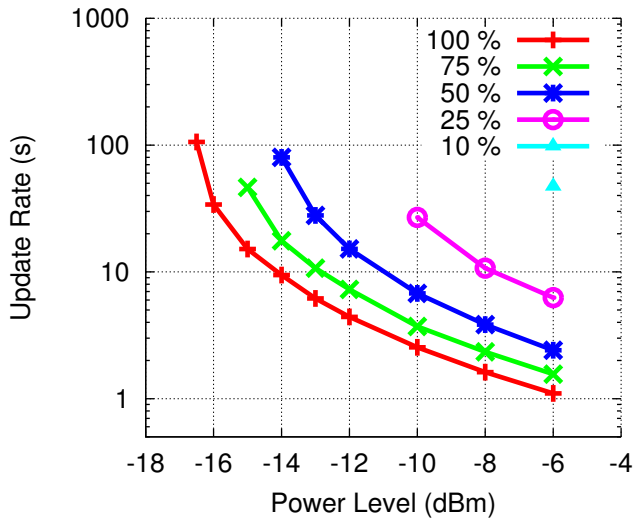


Fig. 11. Update rate of sensor data transmissions using ANT radio protocol as a function of Wi-Fi characteristics.

D. Sensor update rate as a function of Wi-Fi characteristics

Fig. 11 shows the update rate of the temperature sensor as a function of input power and duty cycle. It can be seen that when the input power and duty cycle is high, the update rate from the wearable platform is in the order of few seconds but as the average available power decreases, a consequence of either lower input power and/or lower duty cycle, the update rate of the temperate also decreases to one reading per 100 seconds. For typical sensor applications, a data point every couple of minutes is sufficient and hence, Wi-Fi harvesting is a suitable solution.

E. Operation of wearable platform with a Smartphone

Finally, we evaluate the full wearable platform performance including the antenna with a smartphone as the power source. Since the performance of the harvester is a function of input power and duty cycle of Wi-Fi transmissions, it is imperative that the Wi-Fi power source, the smartphone, is configured to transmit at high duty cycle and high transmit power. However, as noted before, smartphones have reduced transmit

power. We conducted experiments in anechoic chamber and laboratory setting to ascertain the per packet average transmit power of Wi-Fi transmissions. We placed a Wi-Fi antenna connected to a high frequency oscilloscope and measured the power received from the smartphone at different distances. We de-embedded the antenna gains and used Friis equation to experimentally ascertain that the per packet average transmit power of typical smartphones (including antenna and enclosure losses) is around 2 dBm.

Next we maximize the duty cycle by configuring the smartphone as a Wi-Fi hotspot. We connect another device to the hotspot and stream a Youtube video from the hotspot which results in high duty cycle Wi-Fi transmissions (about 75%) from the smartphone. In our experiments, we achieved a maximum operating distance of 11.5 cm between the smartphone acting as a Wi-Fi hotspot and the developed Wi-Fi powered wearable platform. Note that instead of using the smartphone as a hotspot, an application on a smartphone can also ensure high duty cycle Wi-Fi transmissions.

V. DISCUSSION AND FUTURE WORK

We have designed and evaluated the *first Wi-Fi powered battery-free wearable radio platform*, which operates in close proximity of a smartphone. Although the current implementation can operate only up to a distance of 11.5 cm from a typical smartphone (with 2 dBm Wi-Fi transmit power), a Wi-Fi powered radio has the potential to be a battery-free solution for a range of use cases. For example, the current prototype implementation could be used to power and communicate with a battery-free EMG sensor strapped to the knee from a smartphone kept in the pocket of the user. However, to enable a truly ubiquitous battery-free wearable radio platform, the platform should operate at longer ranges without significantly impacting the usability and battery-life of the smartphone.

A. Improving the operating range

The operating range can be increased by improving the sensitivity of the RF harvester and/or increasing the output power of the source i.e. the smartphone. The sensitivity of the RF harvester can be increased by using an integrated on chip rectifier, lower threshold diodes in rectifier, lower V_{in} threshold DC-DC converter and by reducing the leakage power of the platform. Additionally, the Wi-Fi chipsets used in typical smartphones are rated to output up to 20 dBm. Software modifications to the phone can increase the Wi-Fi transmit power to 20 dBm and the operating range of the current prototype can be extended to 92 cm.

B. Usability and impact on the battery life of smartphone

In addition to increasing the operating range, power delivery should not degrade the usability and battery life of the smartphone. Although, the power consumption of smartphones is a complex function of power profile of chipsets, operating system, application software and user behavior, we will investigate the performance under some basic set of assumptions. Typical smartphones have a 3.8 V, 2200-4000 mAh battery,

which can last up to 12 hours on a single charge. Wi-Fi chipsets on smartphones have an energy efficiency of $1.3 \mu\text{J}/\text{bit}$, which translates to an average power consumption of about 100 mW for 2 dBm Wi-Fi transmission [30]. Hence, delivering power using Wi-Fi reduces the battery life of the smartphone by about 8-15 %. However, we note that the above analysis only includes the power consumption of the Wi-Fi chipset and not the account the power overhead associated with CPU, memory, etc. Additionally, since the sensor update rate varies with duty cycle (Fig. 11), the duty cycle of Wi-Fi transmissions from the smartphone can be adapted with distance and application needs to conserve the battery life of the smartphone. The focus of this work is the design of the Wi-Fi harvesting platform. Design and evaluation of smartphone performance acting as a Wi-Fi power source is a topic of future work.

Finally, we also note that the communication protocol can be optimized to meet the specific needs of the application and the power requirements of the radio. For example, instead of transmitting every sensor reading, the platform can periodically sense, store data in memory and transmit the aggregated back to the access point in burst. The design and optimization of the communication protocol is also a topic of future research.

VI. CONCLUSION

In this work, we have developed the first Wi-Fi powered radio platform. We presented the design and analysis of the Wi-Fi harvesting chain and studied the impact of wide band nature of Wi-Fi transmissions, OFDM modulation and duty cycle on the performance of the harvester. Our prototype achieves a sensitivity of -16.5 dBm with 100 % duty cycle Wi-Fi transmissions for a target output voltage of 2.05 V and $2.5 \mu\text{W}$ platform leakage at the output. The developed Wi-Fi powered radio platform can operate up to a distance of 11.5 cm from a 2 dBm Wi-Fi transmitter (on a typical smartphone).

REFERENCES

- [1] M. Billinghurst and T. Starner, "Wearable devices: new ways to manage information," *Computer*, vol. 32, no. 1, pp. 57–64, 1999.
- [2] (2014) Jawbone. [Online]. Available: <https://jawbone.com>
- [3] (2014) Fitbit. [Online]. Available: <http://www.fitbit.com/>
- [4] (2014) Apple watch. [Online]. Available: <https://www.apple.com/watch/>
- [5] J. G. Koomey, S. Berard, M. Sanchez, and H. Wong, "Implications of historical trends in the electrical efficiency of computing," *Annals of the History of Computing, IEEE*, vol. 33, no. 3, pp. 46–54, 2011.
- [6] R. Bogue, "Mems sensors: past, present and future," *Sensor Review*, vol. 27, no. 1, pp. 7–13, 2007.
- [7] J. A. Paradiso and T. Starner, "Energy scavenging for mobile and wireless electronics," *Pervasive Computing, IEEE*, vol. 4, no. 1, pp. 18–27, 2005.
- [8] R. J. Vullers, R. Schaijk, H. J. Visser, J. Penders, and C. V. Hoof, "Energy harvesting for autonomous wireless sensor networks," *Solid-State Circuits Magazine, IEEE*, vol. 2, no. 2, pp. 29–38, 2010.
- [9] V. Raghunathan, A. Kansal, J. Hsu, J. Friedman, and M. Srivastava, "Design considerations for solar energy harvesting wireless embedded systems," in *Proceedings of the 4th international symposium on Information processing in sensor networks*. IEEE Press, 2005, p. 64.
- [10] J. Kymissis, C. Kendall, J. Paradiso, and N. Gershenfeld, "Parasitic power harvesting in shoes," in *Wearable Computers, 1998. Digest of Papers. Second International Symposium on*. IEEE, 1998, pp. 132–139.
- [11] S. R. Anton and H. A. Sodano, "A review of power harvesting using piezoelectric materials (2003–2006)," *Smart materials and Structures*, vol. 16, no. 3, p. R1, 2007.
- [12] A. Sample and J. R. Smith, "Experimental results with two wireless power transfer systems," in *Radio and Wireless Symposium, 2009. RWS'09. IEEE*. IEEE, 2009, pp. 16–18.
- [13] Y. Ramadass and A. Chandrakasan, "A batteryless thermoelectric energy-harvesting interface circuit with 35mv startup voltage," in *Solid-State Circuits Conference Digest of Technical Papers (ISSCC), 2010 IEEE International*, Feb 2010, pp. 486–487.
- [14] A. N. Parks, A. P. Sample, Y. Zhao, and J. R. Smith, "A wireless sensing platform utilizing ambient rf energy," in *Biomedical Wireless Technologies, Networks, and Sensing Systems (BioWireless), 2013 IEEE Topical Conference on*. IEEE, 2013, pp. 154–156.
- [15] V. Liu, A. Parks, V. Talla, S. Gollakota, D. Wetherall, and J. R. Smith, "Ambient backscatter: wireless communication out of thin air," in *Proceedings of the ACM SIGCOMM 2013 conference on SIGCOMM*. ACM, 2013, pp. 39–50.
- [16] S. Lönn, U. Forssen, P. Vecchia, A. Ahlbom, and M. Feychting, "Output power levels from mobile phones in different geographical areas; implications for exposure assessment," *Occupational and Environmental Medicine*, vol. 61, no. 9, pp. 769–772, 2004.
- [17] S. H. Han and J. H. Lee, "An overview of peak-to-average power ratio reduction techniques for multicarrier transmission," *Wireless Communications, IEEE*, vol. 12, no. 2, pp. 56–65, 2005.
- [18] M. S. Trotter, J. D. Griffin, and G. D. Durgin, "Power-optimized waveforms for improving the range and reliability of rfid systems," in *RFID, 2009 IEEE International Conference on*. IEEE, 2009, pp. 80–87.
- [19] A. M. Hawkes, A. R. Katko, and S. A. Cummer, "A microwave metamaterial with integrated power harvesting functionality," *Applied Physics Letters*, vol. 103, no. 16, p. 163901, 2013.
- [20] H. Gao, P. Baltus, R. Mahmoudi, and A. van Roermund, "2.4 ghz energy harvesting for wireless sensor network," in *Wireless Sensors and Sensor Networks (WiSNet), 2011 IEEE Topical Conference on*. IEEE, 2011, pp. 57–60.
- [21] J. F. Ensworth, S. J. Thomas, S. Y. Shin, and M. S. Reynolds, "Waveform-aware ambient rf energy harvesting," in *RFID (IEEE RFID), 2014 IEEE International Conference on*. IEEE, 2014, pp. 67–73.
- [22] U. Olgun, C.-C. Chen, and J. L. Volakis, "Efficient ambient wifi energy harvesting technology and its applications," in *Antennas and Propagation Society International Symposium (APSURSI), 2012 IEEE*. IEEE, 2012, pp. 1–2.
- [23] (2011) $\mu\text{pg}2163\text{t}5\text{n}$ by cel. [Online]. Available: <http://www.cel.com/pdf/datasheets/upg2163t5n.pdf>
- [24] (2008) Design note 007 by ti. [Online]. Available: <http://www.ti.com/lit/an/swru120b/swru120b.pdf>
- [25] (2012) Datasheet of sms7630-061 diodes by skyworks. [Online]. Available: http://www.skyworksinc.com/uploads/documents/SMS7630-061_201295G.pdf
- [26] R. M. Fano, "Theoretical limitations on the broadband matching of arbitrary impedances," *Journal of the Franklin Institute*, vol. 249, no. 1, pp. 57–83, 1950.
- [27] (2013) Datasheet of bq25570 by ti. [Online]. Available: <http://www.ti.com/lit/ds/symlink/bq25570.pdf>
- [28] (2014) nrf51422 by nordic. [Online]. Available: <https://www.nordicsemi.com/eng/Products/ANT/nRF51422>
- [29] (2015) Tps780270200ddcr by ti. [Online]. Available: <http://www.mouser.com/ds/2/405/sbvs083e-528045.pdf>
- [30] M. Lauridsen, L. Noël, T. B. Sørensen, and P. Mogensen, "An empirical lte smartphone power model with a view to energy efficiency evolution," *Intel Technology Journal*, vol. 18, no. 1, pp. 172–193, 2014.